JOURNAL OF PROPULSION AND POWER
Vol. 12, No. 4, July–August 1996

Stochastic–Probabilistic Efficiency Enhanced Dispersion Modeling of Turbulent Polydispersed Sprays

Xi-Qing Chen* and José Carlos F. Pereira†
Instituto Superior Técnico, 1096 Lisbon, Portugal

A stochastic–probabilistic, efficiency enhanced dispersion (SPEED) model is developed for the prediction of turbulent two-phase flows. The SPEED model computes both the mean and variance of droplet positions at each Lagrangian integral time step. The mean position is determined with an improved conventional stochastic model, whereas the variance is determined by a newly derived Lagrangian equation with a Lagrangian autocorrelation function. A memoryless Markovian chain is used to determine the autocorrelation function. The distribution of a physical droplet in space is determined with a prescribed probability density function. The efficiency of the SPEED model is that a minimal number of droplet trajectories are required for Lagrangian trajectory computations during which a large amount of smooth noise-free solution can be attained. The developed SPEED model is first validated against a benchmark test where the measured mean-squared dispersion width is available. Then the results include the prediction of a polydispersed turbulent spray with detailed experimental measurements. Numerical results of the SPEED model, using only a total number of 6×10^2 droplet trajectories, are compared with those of a conventional stochastic discrete delta-function model using a total number of 2.1×10^4 trajectories, and with a previous stochastic dispersion-width transport model. It is found that the SPEED model is numerically more efficient than the dispersion-width transport model and needs much fewer number of droplet trajectories than the standard model.

Nomenclature

D_p = droplet diameter
k = turbulent kinetic energy
P = pressure
Re_p = relative Reynolds number, $\rho\sqrt{(\tilde{U}_{pi} - \tilde{U}_i)^2}D_p/\mu$
S_k^p = turbulent energy source from the droplet phase
$S_{U_i}^p$ = momentum sources from the droplet phase
$S_{\overline{u_iu_j}}^p$ = Reynolds-stress sources from the droplet phase
t = time
U = axial gas velocity
V = radial gas velocity
v_{rms} = gas rms velocity, $\frac{2}{3}k$
x = axial coordinate
y = radial coordinate
ε = dissipation rate of k
μ = laminar dynamic viscosity
ρ = density

Subscripts
i, j, k = Cartesian components
p = droplet phase
t = turbulent

Introduction

THE Eulerian–Lagrangian hybrid modeling of dilute two-phase flows has been widely accepted as a powerful and state-of-the art tool to predict a variety of two-phase flows. This hybrid model consists of the Eulerian formulation of the continuous-phase and the Lagrangian formulation of the dispersed-phase where the influence of continuous-phase turbulence on dispersed-phase dispersion is often accounted for by using a stochastic dispersion model. Comprehensive reviews on two-phase flow models can be found in Refs. 1–4, etc.

Since the pioneering work of Yuu et al.[5] and Gosman and Ioannides,[6] many existing Lagrangian stochastic models have followed suit by accounting for the effects of the continuous-phase turbulence on the dispersed-phase dispersion based on the concept of droplet-eddy encounters. Many authors have reported success with these stochastic models in predicting dilute two-phase flows, only to find that detailed inlet conditions play an important role in accurate Lagrangian computations, and that a large number of particle/droplet trajectories are required to achieve a stochastically significant solution. This can be made much clearer through a brief overview of the recent work addressing these two aspects.

Sturgess et al.[7] computed a turbulent hollow-cone spray using a Lagrangian stochastic model. Given no complete inlet conditions from the experiment, they had to artificially specify these inlet conditions required for their numerical predictions. It is found that the prediction of droplet spatial distribution could never be acceptable no matter how they adjusted the inlet specifications. Based on a sensitivity study of the effects of assuming inlet conditions on the prediction of droplet properties, Shuen et al.[8] also demonstrated that the assumption of droplet-phase initial conditions does play an important role in accurate Lagrangian computations. Chen and Pereira[9] used a Eulerian–Lagrangian stochastic model to predict an evaporating spray of Yule et al.[10] without detailed experiments at the inlet. The inlet droplet sizes were assumed to be of the Rosin–Rammler type. It is once again concluded that the prediction of droplet volume concentration was influenced by the assumption of initial droplet sizes at the inlet. Therefore, to get rid of the influence of assuming inlet conditions on numerical predictions, the present study has employed detailed experimental measurements of Chen et al.[11] for a water spray behind a disk. These measurements have provided all of the inlet conditions necessary for Eulerian and Lagrangian computations.

In conventional Lagrangian stochastic computations, particle/droplet properties are determined using an ensemble averaging of many individual particle/droplet trajectories. There-

Received Aug. 4, 1995; revision received Feb. 4, 1996; accepted for publication Feb. 25, 1996.

*Postdoctoral Fellow, Technical University of Lisbon, Mechanical Engineering Department, Av. Rovisco Pais.

†Professor, Technical University of Lisbon, Mechanical Engineering Department, Av. Rovisco Pais. Member AIAA.

fore, a large number of trajectories are required to attain a statistically significant solution. Mostafa et al.[12] found that 10^5 particle trajectories were necessary for their Lagrangian stochastic computation of a monodisperse particle-laden jet. Adeniji-Fashola and Chen[13] reported that smoother profiles of their predicted results can only be achieved with a total number of 9×10^3 computational trajectories for a confined particle-laden jet. To achieve stochastically significant predictions, Bulzan et al.[14] employed a total number of 3.36×10^4 droplet trajectories for a multisized liquid spray. Furthermore, Chang and Wu[15] concluded that a large number of 2×10^4 droplet trajectories are required to reach an invariant solution for a polydispersed turbulent hollow-cone spray. Recently, Chen and Pereira[16] also demonstrated that a total number of 10^4 droplet trajectories are necessary to achieve an invariant solution for a turbulent, polydispersed, evaporating spray. All of these Lagrangian stochastic computations have clarified the fact that a relatively large number of droplet trajectories are necessary, which often requires consuming a great amount of computer CPU time.

This brief review has sufficiently clarified that thousands of droplet trajectories have to be tracked with these conventional stochastic dispersion models, spending a great amount of time in Lagrangian calculations. To overcome the shortcoming of these stochastic dispersion models, Litchford and Jeng[17] developed a stochastic dispersion-width transport (SDWT) model, which aims at providing reduced sampling requirements with minimal numerical noise. The dispersion-width is determined through the linearized droplet equations of motion. However, this model accounts for neither the effects of the anisotropy of gas turbulence on droplet dispersion nor the effects of droplet drift correction. Moreover, an unknown constant accouting for undersampling has to be estimated. Chen and Pereira[18] modified this SDWT model to include these effects. This modified SDWT model was successfully employed to predict a turbulent evaporating spray. It is found that a fewer number of droplet trajectories could be used to achieve smooth profiles of predictions than the conventional stochastic model. Nevertheless, the SDWT model, as seen later, requires too many time-consuming, repeated summing operations, apart from additional computer memory to store the flow property of each droplet-encountered turbulent eddy. As a result, this SDWT model, even though it requires tracking a few numbers of droplet trajectories, still spends much time on computing the turbulence-induced dispersion width where many operations of repeated summations are necessary.

The objective of the present study is to develop a stochastic–probabilistic efficiency enhanced dispersion (SPEED) model for efficient Lagrangian trajectory calculations. The SPEED model adopts the memoryless Markovian-chain to determine a Lagrangian autocorrelation function, which is, in turn, used to determine a dispersion width. Different from the SDWT model, the SPEED model employs an equation governing the change in the dispersion width at each time step. For this reason, it is neither necessary to perform repeated summing operations or to store the additional flow property of each droplet-encountered turbulent eddy, as required by the SDWT model; as a consequence, it offers higher computational efficiency. The developed SPEED model is first validated against a benchmark test of Vames and Hanratty,[19] and then applied to predict a turbulent hollow-cone spray of Chen et al.[11] for which detailed experimental measurements are available. In addition, an assessment of the SPEED model efficiency and accuracy is also carried out by comparing the computer CPU time spent and the extent to which numerical predictions agree with the experimental measurements.

Governing Equations for the Continuous Phase

To adequately predict the anisotropicity of gas turbulence, the Reynolds-stress-transport (RST) model is used to write the governing equations for the continuous gas flowfield. The governing equations for mass and momentum can be written as

$$\frac{\partial \rho U_j}{\partial x_j} = 0 \tag{1}$$

$$\frac{\partial \rho U_i U_j}{\partial x_j} = -\frac{\partial P}{\partial x_i} + \frac{\partial}{\partial x_j}\left(\mu \frac{\partial U_i}{\partial x_j} - \rho \overline{u_i u_j}\right) + S^p_{U_i} \tag{2}$$

where the Reynolds stress $\overline{u_i u_j}$ is governed by its own equation as follows:

$$\frac{\partial}{\partial x_k}(\rho U_k \overline{u_i u_j}) = P_{ij} - \varepsilon_{ij} + \phi_{ij} + D_{ij} + S^p_{\overline{u_i u_j}} \tag{3}$$

where P_{ij}, ε_{ij}, ϕ_{ij}, and D_{ij} are the generation, dissipation, pressure-strain correlation, and diffusion terms, respectively. The source terms $S^p_{U_i}$, $S^p_{\overline{u_i u_j}}$, are from the two-phase interactions. The determination of these sources can be found elsewhere.[9,20] The other terms on the right-hand side of Eq. (3) are determined as follows:

$$P_{ij} = -\rho \overline{u_j u_k} \frac{\partial U_i}{\partial x_k} - \rho \overline{u_i u_k} \frac{\partial U_j}{\partial x_k}, \quad \varepsilon_{ij} = \frac{2}{3}\rho \varepsilon \delta_{ij} \tag{4a}$$

$$D_{ij} = \frac{\partial}{\partial x_k}\left[\left(\mu \delta_{mk} + \rho C_s \frac{k}{\varepsilon} \overline{u_k u_m}\right) \frac{\partial \overline{u_i u_j}}{\partial x_m}\right] \tag{4b}$$

The pressure-strain correlation term of ϕ_{ij} is given by

$$\phi_{ij} = -C_1 \rho \frac{\varepsilon}{k}\left(\overline{u_i u_j} - \frac{2}{3} k \delta_{ij}\right) - C_2\left(P_{ij} - \frac{2}{3} G \delta_{ij}\right) \tag{5}$$

where the production $G = P_{kk}/2$. Finally, the equation governing the dissipation rate of the turbulent kinetic energy reads

$$\frac{\partial}{\partial x_j}(\rho U_j \varepsilon) = \frac{\partial}{\partial x_j}\left(\mu \frac{\partial \varepsilon}{\partial x_j} + C_\varepsilon \rho \frac{k}{\varepsilon} \overline{u_i u_j} \frac{\partial \varepsilon}{\partial x_i}\right) + \frac{\varepsilon}{k}(C_{\varepsilon 1} G - C_{\varepsilon 2} \rho \varepsilon) + C_{\varepsilon 3} \frac{\varepsilon}{k} S^p_k \tag{6}$$

where the droplet–gas interaction term is given by

$$S^p_k = \tfrac{1}{2} S^p_{u_j u_j} \tag{7}$$

The modulation of the droplet phase on the turbulence of the gas phase has been accounted for by following Berlemont et al.[21] The RST model constants are given as follows: (C_s, C_1, C_2, $C_{\varepsilon 1}$, $C_{\varepsilon 2}$, and $C_{\varepsilon 3}$) = (0.22, 1.8, 0.6, 1.45, 1.9, and 1.1).

Equations of Motion for the Dispersed Phase

In the framework of Lagrangian formulation, the equation of motion for each of the droplet parcels can be written as

$$\frac{d\tilde{U}_{pi}}{dt} = \frac{\tilde{U}_i - \tilde{U}_{pi}}{\tau_p} + F_{pi} \tag{8}$$

where $\tilde{U}_i = U_i + u_i$ is the instantaneous gas velocity, and F_{pi} is an external force. The relaxation time of droplets τ_p is defined as

$$\tau_p = \frac{\rho_p D_p^2}{18 \mu f_p} \tag{9}$$

where the drag correction coefficient f_p is determined by

$$f_p = 1 + 0.15 Re_p^{0.687} \qquad (0 < Re_p < 1 \times 10^3) \tag{10}$$

The droplet trajectories are computed by

$$\frac{dx_{pi}}{dt} = \tilde{U}_{pi} \tag{11}$$

Note that the trajectories determined by Eq. (11) represent the droplet mean positions in the following stochastic–probabilistic efficiency enhanced model.

SPEED Modeling of Droplet Dispersion

It is well known that in conventional Lagrangian stochastic models either droplet properties or droplet sources determined at each Lagrangian time step represent the ones only at the current droplet positions corresponding to a point in space. The distribution of a physical droplet in space with these stochastic models is actually characterized by a discrete delta-function distribution. Therefore, these models are called stochastic discrete-delta function (SDDF) models. It is because of this characteristic of the SDDF models that statistically smooth profiles of predictions can only be obtained through tracking a relatively large number of droplet trajectories. As mentioned in the introduction, many researchers have reported a success with the SDDF models, only to find that thousands of trajectories are required. To bring these SDDF models to industrial applications of engineering significance, obviously an efficient stochastic dispersion model is sought, which should be able to offer high computational efficiency, but reduce numerical noise to a minimum. It is to this end that a SPEED model is developed in this article. The SPEED model developed here is based upon an assumed premise that droplet mean positions are determined with a conventional SDDF model while another equation of mean-squared dispersion width is simultaneously solved in Lagrangian trajectory computations. This dispersion width is then used to determine the distribution of a physical droplet in time and space according to a prescribed probability density function (PDF). Therefore, the equation governing the mean-squared dispersion width should be derived. In what follows, the development of the SPEED model is described.

According to the definition of mean-squared dispersion width, the radial dispersion variance can be determined as follows:

$$\frac{d\sigma_r^2}{dt} = \frac{d\overline{r'^2}}{dt} = 2\overline{r'\frac{dr'}{dt}} = 2\overline{\int_0^t v(t)v(t_1)\,dt_1} = 2\int_0^t \overline{v(t)v(t_1)}\,dt_1 \tag{12}$$

where the overbar represents ensemble averaging, $\overline{v(t)v(t_1)}$ the radial gas fluctuating velocity correlation in the time interval between t and t_1, which can be determined with resort to a Lagrangian autocorrelation function, defined by

$$R_L(t_1, t) = \frac{\overline{v(t)v(t_1)}}{\overline{v^2(t)}} \tag{13}$$

where $\overline{v^2(t)}$ represents the radial component of gas normal stresses at t, corresponding to the droplet current position. It can be obtained by interpolating the RST predictions to the current droplet positions. On the assumption of a homogeneous turbulent flowfield, the previous equation can be simplified as

$$R_L(t_1, t) = R_L(t_1 - t) = R_L(\Delta t) = \frac{\overline{v(t)v(t + \Delta t)}}{\overline{v^2(t)}} \tag{14}$$

where the velocity correlation can be appoximated using the single time-step Markovian chain. As a result, the Lagrangian autocorrelation function can be determined by

$$R_L(\Delta t) = \exp[-(\Delta t/T_L)] \tag{15}$$

where T_L is the Lagrangian integral time constant, and is computed by

$$T_L = 0.3(k/\varepsilon) \tag{16}$$

Finally, the equation governing the radial dispersion width σ_r can be written as

$$\frac{d\sigma_r^2}{dt} = 2\overline{v^2}T_L\left[1 - \exp\left(-\frac{\Delta t}{T_L}\right)\right] \tag{17}$$

which can be integrated to yield the evolving dispersion width along droplet trajectories. When a droplet encounters a turbulent eddy, T_L can be determined with the gas-phase RST model predictions, and is kept fixed within the period of droplet–eddy interaction time. As a result, it follows that

$$\sigma_r^2(t) \approx \sigma_r^2(t - \Delta t) + 2\overline{v^2}T_L\Delta t\{1 - \exp[-(\Delta t/T_L)]\} \tag{18}$$

Note that in deriving Eq. (17) it has been implicitly assumed that the dispersion width of a droplet is equal to that of a fluid tracer. Even though this assumption is not valid for large droplets, it is an approximate way to obtain the droplet trajectory variance. To obtain the instantaneous gas velocity in Eq. (8), it is necessary to determine the fluctuating velocity. Most reseachers are using the stochastic dispersion model of Gosman and Ioannides.[6] This model is, however, essentially an isotropic stochastic dispersion model that fails to account for the effects of the anisotropy of gas turbulence on droplet dispersion. Given reliable information of the anisotropy of gas turbulence by the Reynolds stress model, this conventional discrete delta-function model was recently improved by Chen and Pereira[18] to account for the anisotropic effects of gas turbulence on droplet dispersion. In the improved model, the gas fluctuating velocity is given by

$$u_i = \sqrt{\overline{u_j^2}}\xi_j\delta_{ij} \tag{19}$$

where ξ_j is a Gaussian random variable having zero mean and unity deviation. Note that the normal stresses are used here, instead of $2k/3$. To overcome the buildup of mass-flux predictions near the centerline far downstream as observed by Adeniji-Fashola and Chen[13] and Chen and Pereira,[20] Chen and Pereira[16] further developed an approach to determining the transverse component in Eq. (19) by

$$\xi_v = \xi_v' + (\sqrt{\overline{v^2}}/r_p)\tau_p\alpha_p \tag{20}$$

where ξ_v' is a Gaussian variable having zero mean and unity deviation, r_p the droplet radial mean position determined with Eq. (11), and α_p a controlling parameter, being either zero or unity, to switch on or off this modification. This method has been proved very effective in eliminating the aphysical accumulation of mass-flux predictions.[16] Note that Eqs. (19) and (20) are employed to determine the fluctuating gas velocities in Eq. (8).

For the sake of ensuing comparison, the stochastic dispersion-width transport (SDWT) model[22] is also briefly described. The SDWT model determines a dispersion-width, induced by gas turbulence after each droplet–eddy interaction, which is then used as the standard deviation of the computational parcel's PDF after each interaction. Normalized by the total number of computational parcels, the overall mean square dispersion corresponding to the variance of the parcel PDF after nth interaction is determined by

$$\sigma_r = \frac{K}{\sqrt{N_{cp}}}\sqrt{\sum_{k=1}^{n}(v_{rms}T_k)^2} \tag{21}$$

where K is introduced as a correction factor to account for

undersampling, N_{cp} the number of computational parcels, and T_k essentially an effective time constant for turbulent dispersion that accounts for the influence of the kth interaction on dispersion after nth eddy, given by

$$T_k = \Delta t_k - \tau_{pk}A_k + \left[A_k \sum_{i=k+1}^{n} \begin{cases} \tau_{pi}A_i \exp\left(-\sum_{j=k+1}^{i-1} \frac{\Delta t_j}{\tau_{pj}}\right) & i > k+1 \\ \tau_{pi}A_i & i = k+1 \end{cases} \quad k < n \right] \quad (22a)$$

$$+ \left[0 \quad k = n \right]$$

with A_k given by

$$A_k = 1 - \exp[-(\Delta t_j/\tau_{pj})] \quad (22b)$$

The previous normalization procedure requires determining an unknown constant K, which depends on different flow problems. The effects of K on predictions have been studied by Chen and Pereira[23] for the present spray, and it is found that $K = 4$ is an appropriate value; therefore, this value is still adopted here for the spray prediction. Of particular note is that there are too many repeated computations in determining the dispersion width with the SDWT [see Eqs. (21) and (22)]. This not only consumes a lot of computer CPU time but also requires a large amount of computer memory for each droplet–eddy encounter. Moreover, K has to be estimated for the flow to be investigated. However, we can easily find, by comparing Eq. (18) with Eq. (21), that computation of dispersion width with Eq. (18) only requires storing the dispersion width at last time step; moreover, it also avoids many repeated summing operations in Eqs. (21) and (22). Hence, Eq. (18) offers higher efficiency than Eqs. (21) and (22). The accuracy of these two models will be assessed in terms of the comparison with the experimental measurements.

Given droplet position mean and variance, we are now in a position to compute droplet probability distribution in terms of PDF. The appropriate PDF may be Gaussian; however, an isosceles triangle PDF is used in the present study to substitute the Gaussian PDF for simplification. The isosceles probability distribution function is given by

$$f(r) = \begin{bmatrix} 0 & r \le r_p - w \\ \dfrac{r - r_p + w}{w^2} & r_p - w < r \le r_p \\ -\dfrac{r - r_p - w}{w^2} & r \ge r_p + w \end{bmatrix} \quad (23)$$

where $w = 2\sqrt{3}\sigma_r$ is the PDF halfwidth, and r is the radial coordinate. Given the PDF, the probability distribution can be determined. Depending on different situations, Eq. (23) can be integrated for axisymmetric flows to give corresponding probability distributions at a radial position r. Consequently, it follows[22] that

$$P(r) = \begin{bmatrix} P_A & 0 < r < w - r_p \\ P_C & w - r_p < r < r_p \\ P_D & w - r_p < r < w + r_p \\ 1 & r \ge w + r_p \end{bmatrix} \quad \text{for} \quad w/2 < r_p < w \quad (24a)$$

$$P(r) = \begin{bmatrix} P_A & 0 < r < r_p \\ P_B & r_p < r < w - r_p \\ P_D & w - r_p < r < w + r_p \\ 1 & r \ge w + r_p \end{bmatrix} \quad \text{for} \quad 0 < r_p < w/2 \quad (24b)$$

$$P(r) = \begin{bmatrix} 0 & 0 < r < r_p - w \\ P_C & r_p - w < r < r_p \\ P_E & r_p < r < w + r_p \\ 1 & r \ge w + r_p \end{bmatrix} \quad \text{for} \quad r_p > w \quad (24c)$$

where $P(r)$ represents the probability of having a droplet at r, r_p the droplet current position obtained with Eq. (11). Terms P_A, P_B, P_C, P_D, and P_E are computed as follows:

$$P_A = \frac{6|w - r_p|r^2}{-2r_p^3 + (w + r_p)^3 + |w - r_p|^3}$$

$$P_B = \frac{-4r^3 + 6wr^2 - 2r_p^3}{-2r_p^3 + (w + r_p)^3 + |w - r_p|^3}$$

$$P_C = \frac{2r^3 + 3|w - r_p|r^2 + |w - r_p|^3}{-2r_p^3 + (w + r_p)^3 + |w - r_p|} \quad (25)$$

$$P_D = \frac{-2r^3 + 3(w + r_p)r^2 - 2r_p^3 + |w - r_p|^3}{-2r_p^3 + (w + r_{\bar{p}})^3 + |w - r_p|^3}$$

$$P_E = \frac{2r^3 - 3(w + r_p)r^2 - 2r_p^3 + |w - r_p|^3}{-2r_p^3 + (w + r_p)^3 + |w - r_p|^3}$$

Determination of Droplet Properties

In Lagrangian computations, either droplet properties or sources obtained at each time step represent the ones at droplet mean positions, and should be distributed using the assumed isosceles PDF in terms of the current dispersion width. Therefore, any number-averaged droplet property (e.g., droplet velocity and diameter) at a Eulerian control volume P, has to take into consideration the spatial probability distribution, yielding

$$\overline{\Phi_P} = \sum_{k=1}^{M} \Phi_k \dot{N}_k \Delta t_k [P_k(r_n) - P_k(r_s)] \Big/ \sum_{k=1}^{M} \dot{N}_k \Delta t_k [P_k(r_n) - P_k(r_s)] \quad (26)$$

where the subscript k represents the kth droplet parcel crossing the Eulerian control volume P as shown in Fig. 1, and M is the total number of droplet trajectories crossing the control volume. Note that M depends on the total number of droplet trajectories used at the inlet. In Eq. (26) r_n and r_s denote the north and south surfaces of the control volume, respectively. The probability of $P(r)$ in Eq. (26) is determined by Eq. (24). Similarly, the droplet sources can also be distributed into Eulerian control volumes, except that these terms are calculated using the absolute number of droplets in the control volume. It should be stressed that a drift correction has to be used for correct prediction of mass fluxes for axisymmetric two-phase flows; otherwise predicted mass fluxes tend to accumulate near the centerline far downstream.[20] Therefore, the drift correction method developed by Chen and Pereira[16] has been employed in the present study.

Validation Against a Benchmark Test

To preliminarily validate the SPEED model, the experiment performed by Vames and Hanratty[19] is used here as a benchmark test. The experiment was conducted in a 5.08-cm-diam

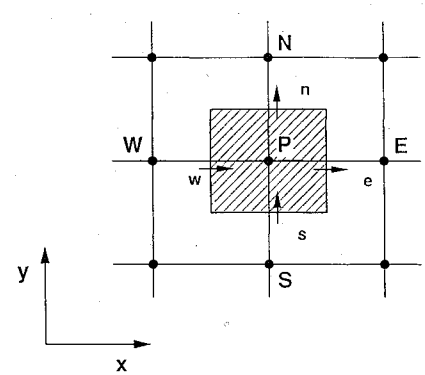

Fig. 1 Typical Eulerian control volume.

vertical pipeline where air flowed downward. A continuous stream of water droplets with a uniform size of 50 μm was injected down the centerline of the pipe. The experimental setup was arranged so that the water droplets were injected vertically downwards. In such a way, the gravity has no component in the radial direction; therefore, the effects of gravitational term on the radial mean-squared displacement can be ruled out. In the stochastic modeling of the water-droplet dispersion, the gas-phase field, i.e., the mean velocity profile, the turbulent properties, etc., were prescribed using the measurements of Laufer[24] for the fully developed pipe flow. The centerline gas velocity is 11.2 m/s. The monosized water droplets were injected downward with a mean streamwise velocity of 8.3 m/s. The initial radial and tangential mean velocities were zero. A total number of 1.5×10^4 and 10 droplet trajectories are used, respectively, for the SDDF model and SPEED model. The radial mean-squared dispersions in the Lagrangian tracking were calculated in the experimentally prescribed time intervals to carry out a direct comparison between the measurements and predictions.

Figure 2 shows the comparison of the predicted mean-squared dispersions of the SDDF and SPEED models with the experimental measurements. It can be seen that both of these two model predictions agree well with the measurements; however, of particular note is that a much fewer number of droplet trajectories has been employed for the SPEED models.

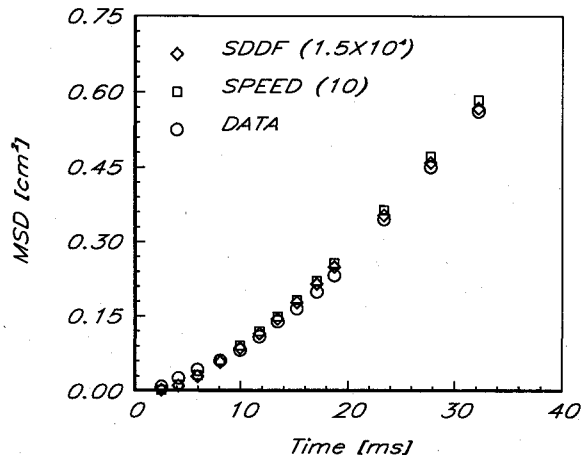

Fig. 2 Comparison of mean-squared dispersion.

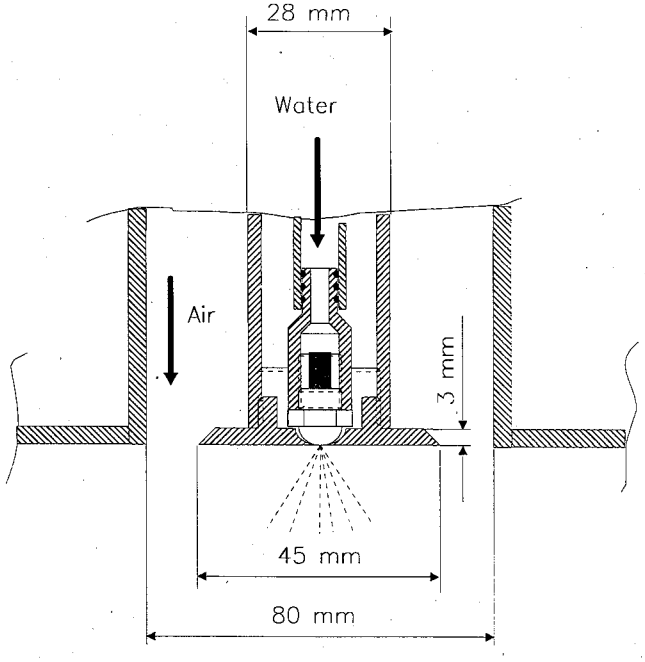

Fig. 3 Experimental spray configuration.

Application to a Turbulent Multisized Spray

To further see the capability of the SPEED model to predict turbulent sprays, a nonevaporating, polydispersed, turbulent spray of Chen et al.[11] is considered here for the SPEED model validation, even though other measurements are also available.[14,25] The spray configuration is shown in Fig. 3, where air was discharged downward through a nozzle with a diameter of 80 mm surrounding a disk with a diameter of 45 mm. A spray nozzle was located in the center of the disk. Under a pressure of 4 bar, the nozzle creates droplet sizes ranging from 10 to 100 μm. The liquid mass loading at the inlet was about 1%. This clearly shows that the spray was very dilute.

The finite volume method is employed to solve the Eulerian equations together with a staggered grid arrangement. The

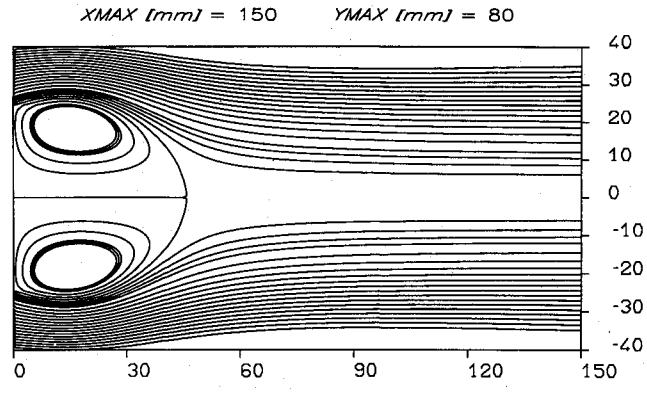

Fig. 4 Gas-phase flow streamlines.

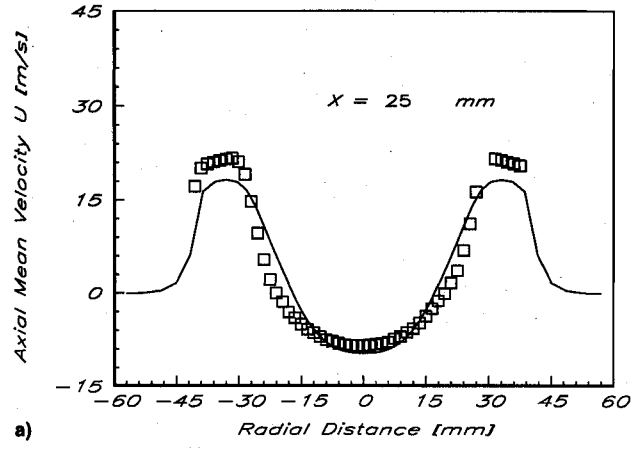

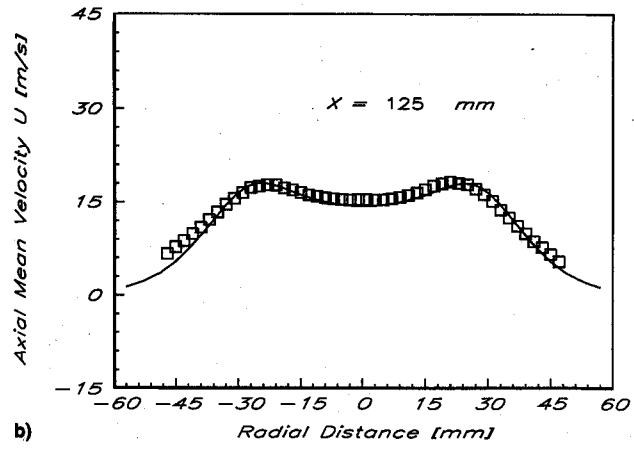

Fig. 5 Comparison of axial gas mean velocity.

third-order discretization of the QUICK algorithm was used for convection discretization. The initial conditions at the inlet were obtained by interpolating the experimental measurements.[11] The Lagrangian equations are solved by integrating the ordinary-differential equations. A very small time step is used for integration. The time step is subject to limitation of several time scales, such as grid time, eddy-life time, and eddy-transit time, etc. The initial droplet-size distribution of the spray is specified according to the experimentally measured PDF to obtain an adequate number of discrete parcels, each of which represents a set of droplets having the same size and initial conditions. The droplet source terms determined in Lagrangian computations are distributed into gas Eulerian equations according to the residence time of droplets in an Eulerian control volume and the probability distribution. The gas properties at current droplet positions are interpolated using an accurate second-order algorithm similar to that used by Rangel and Sirignano.[26] Experimental measurements indicate that the spray could be satisfactorily considered axisymmetric. Therefore, only half of the flow domain was considered in the numerical calculations. For the present unconfined spray, a computational domain of 350 mm axially by 95 mm radially is used to fully cover the jet expansion. On the free boundary, free-entrainment conditions are employed for the continuous phase.[27] In Lagrangian trajectory calculations, the tracking procedure stops, if a droplet leaves the computational domain. The present numerical computations were performed using a grid of 73 × 71 in the axial and radial directions, respectively. Refined grids were distributed in the region close to the nozzle to resolve the flow near the nozzle.

Detailed experimental measurements of radial profiles were performed at X = 4, 10, 20, 30, 40, 60, and 100 mm. The first radial profile at X = 4 mm was used as the initial conditions required for the numerical computations. The remaining profiles were used to assess the numerical results. The first profile of measurements provides such detailed droplet properties as droplet sizes and their corresponding PDF, mean and rms velocities for each of the droplet sizes, mass fluxes, and droplet mean diameters at each measured point.

Figure 4 shows the gas-phase streamlines. It can be seen that strong flow recirculations are present in the region close to the inlet. Droplet dispersion behavior is clearly influenced by the gas flow within this recirculating region. In the following comparisons, therefore, two profiles at X = 40 and 100 mm are chosen to represent the ones within and away from the recirculating region. Compared in Figs. 5a and 5b are the radial profiles of axial gas mean velocity. It can be seen that the predictions agree satisfactorily with the measurements. Figures 6a and 6b show the predicted and measured axial gas fluctuating velocity. It is evident that some discrepancies occur between the predictions and measurements. Similar behavior can also be observed in Figs. 7a and 7b for radial gas fluctuating velocity. The predicted two components of gas fluctuating velocity at X = 125 mm rather qualitatively than quantitatively agree with the measurements. This is probably attributed to the standard RST model used for such a flow with steep gradient.

Shown in Fig. 8 are the predictions of the droplet axial mean velocity and mass flux obtained with the SPEED and SDDF models using a total number of 6 × 10^2 droplet trajectories. It is clearly observed that a lot of numerical noise exists in the SDDF model predictions, especially in the region close to the centerline. This clarifies that a larger number of droplet trajectories are required to achieve a statistically significant solution for the SDDF model. To this end, a larger number of 2.1 × 10^4 droplet trajectories are tracked with the SDDF model. The results are compared with those using a total number of 6 × 10^2 droplet trajectories. It is found that the numerical noise is substantially reduced because of the larger number of droplet

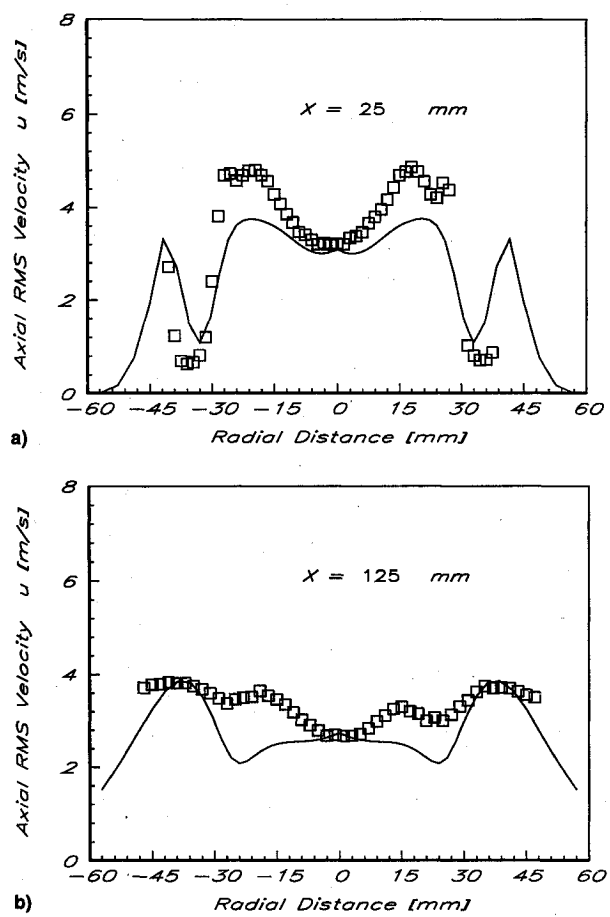

Fig. 6 Comparison of axial gas fluctuating velocity.

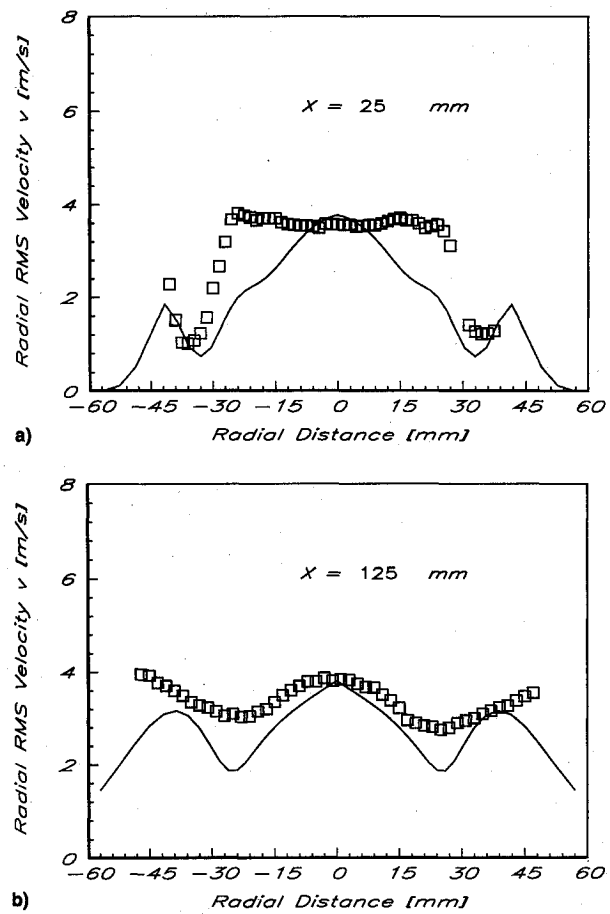

Fig. 7 Comparison of radial gas fluctuating velocity.

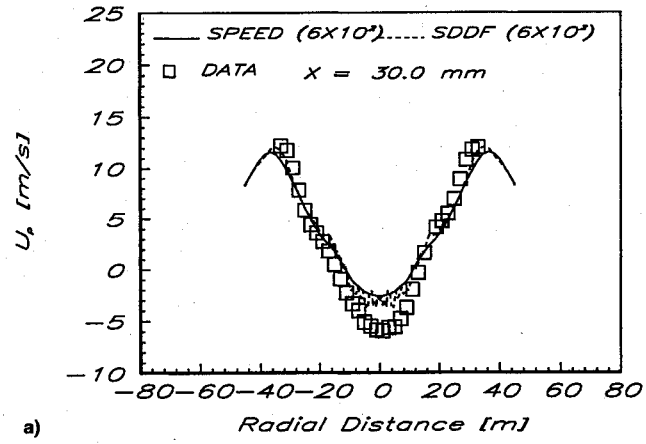

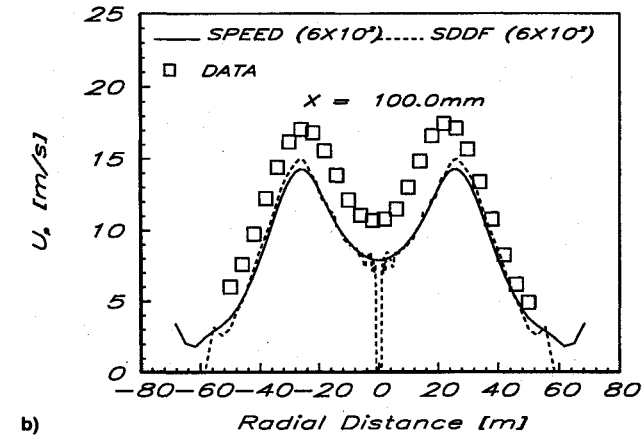

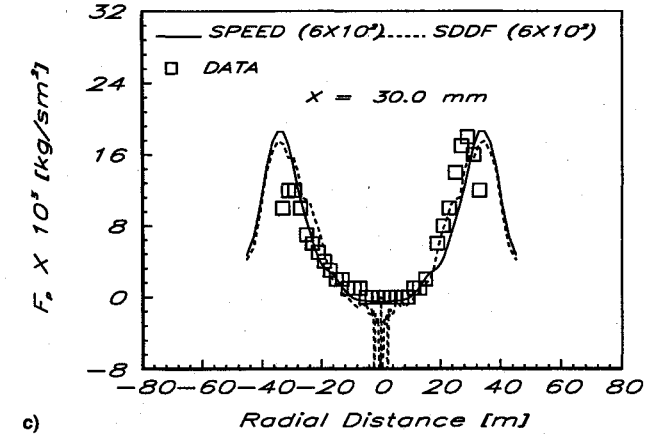

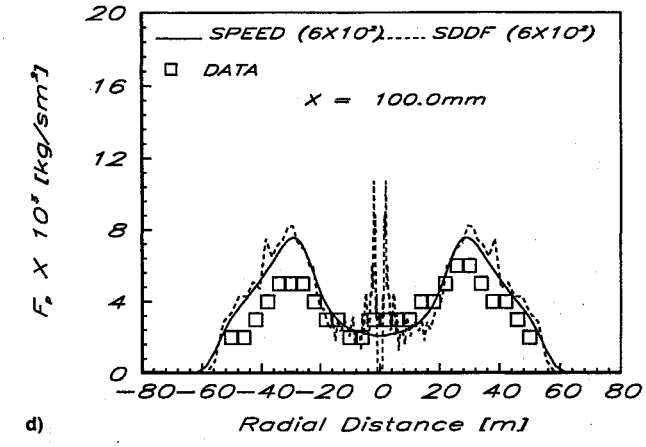

Fig. 8 SPEED and SDDF model predictions with 6 × 10^2 trajectories: a), b) droplet axial mean velocity and c), d) droplet mass flux.

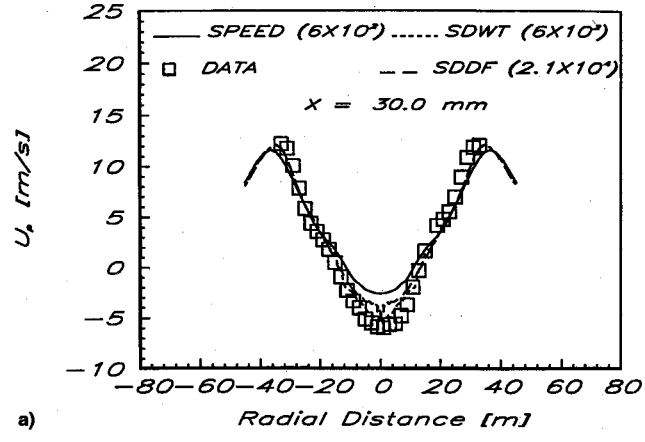

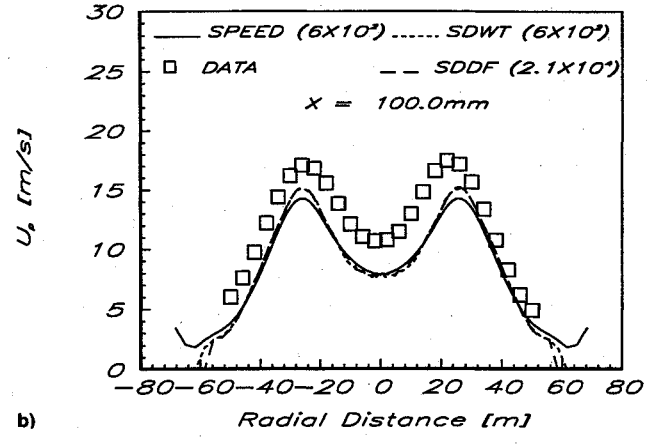

Fig. 9 Droplet axial mean velocity predicted with three models.

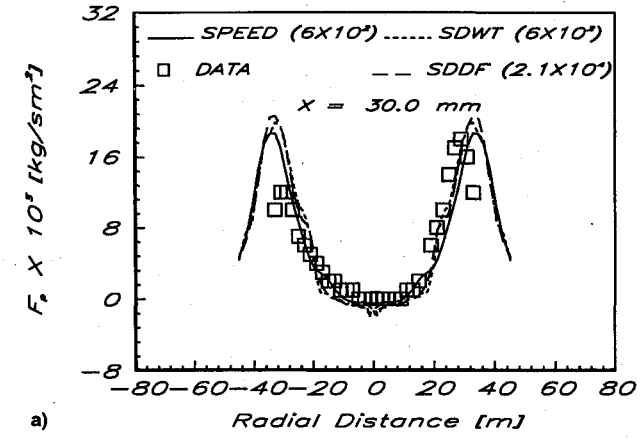

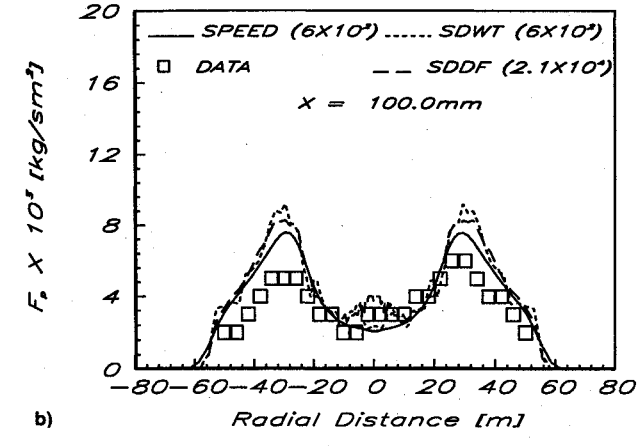

Fig. 10 Droplet mass flux predicted with three models.

trajectories used. Even so, some numerical noise persists in the region close to the centerline where very few droplets are present. In what follows, the SDDF model predictions with the larger number of trajectories are compared with those of the SPEED model using a total number of 6×10^2 droplet trajectories.

The efficiency of the SDWT and SDDF models has been examined by Chen and Pereira[23] according to the CPU time spent in these two model computations. The computations were performed with a computer DEC Alpha 7610 at IST, Lisbon. It is found that the SDWT model requires about 2 min of CPU time to perform each Lagrangian tracking of 6×10^2 droplet trajectories while the SDDF model requires about 35 min of CPU time for each tracking of 2.1×10^4 trajectories. However, the present SPEED model requires only about 1 min for each tracking of 6×10^2 trajectories. This is clearly demonstrative of high computational efficiency gained with the SPEED model. Even though the SPEED model computes the same number of 6×10^2 droplet trajectories as the SDWT model, it does not require, however, the repeated summing operations in determining the dispersion width. It is because of this fact that higher computational efficiency is offered by the SPEED model. In addition, it is also found that a fewer number of two-way coupling iterations are necessary for final convergence with the SPEED model as compared to the SDDF model. This is because the SPEED model distributes the sources according to the probability distribution, thus yielding smooth sources in Eulerian equations. As a result, the convergence rate of two-phase iterations is sped up with the SPEED model. This favorable behavior of the SPEED model would be very helpful for predicting relatively dense two-phase flows where two-way coupling is pronounced. Bearing in mind the high computational efficiency gained with the SPEED model, we further examine the accuracy of the model in terms of its agreement with the measurements. The numerical comparisons are conducted for the droplet axial mean velocity, diameter, and mass flux.

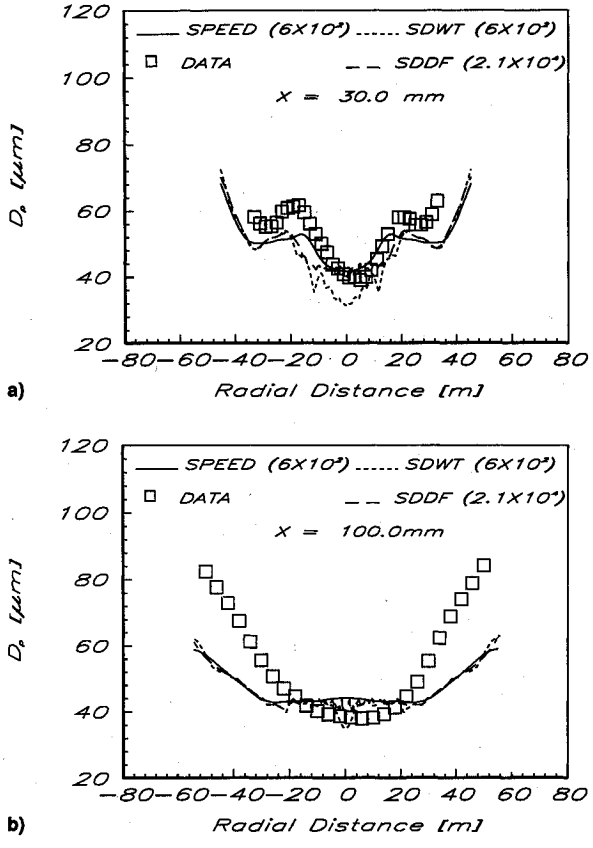

Fig. 11 Droplet mean diameter predicted with three models.

Shown in Figs. 9a and 9b are the profiles of the predicted and measured droplet axial mean velocity at $X = 40$ and 100 mm. Note that the SDWT predictions are also shown here for the sake of a comparative study. It can be seen that the predictions with the SPEED model are much smoother. However, numerical noise close to the centerline exists in the predictions with both the SDWT and SDDF models. The presence of numerical noise in the SDDF model predictions can be made clear in our previous study[11] where droplet trajectories are visualized. It is observed that very few droplets are moving towards the centerline because of the unfavorable influence of flow recirculations. Of particular note is that the SDDF and SDWT predictions are much similar except that relatively smoother profiles are obtained with the SDWT model. This is because the SDWT model adopts the concept of droplet–eddy encounters to compute the dispersion width and the normalizing practice used in Eq. (21), which has substantially reduced the turbulence-induced dispersion width at droplet–eddy encounters.

Shown in Fig. 10 are the profiles of the predicted and measured droplet mass fluxes. Once again, it can be found that computational noise exists in the region close to the centerline in the SDWT and SDDF model predictions. The smoothest profiles are obtained with the SPEED model. Moreover, the SPEED model predictions are still more agreeable with the measurements than the other two models.

The profiles of the predicted and measured droplet number-mean diameters are compared in Fig. 11. It is clearly demonstrated that the SPEED model predictions are much smoother than both the SDWT and SDDF model predictions. In the present computations, no droplet vaporization was considered. This is because the measurements and predictions were concentrated near the inlet, and the latent heat of vaporization for a water droplet is relatively large. This may justify the simplified computations. It can be inferred that the droplet vaporization

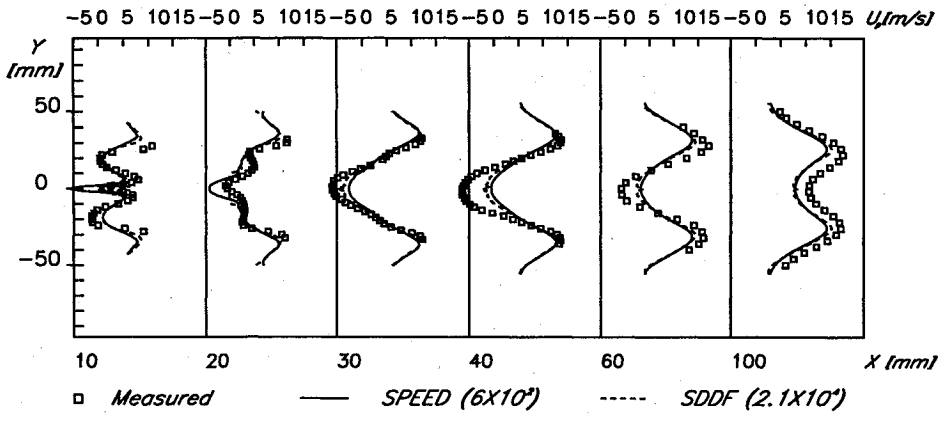

Fig. 12 Comparison of droplet axial mean velocity.

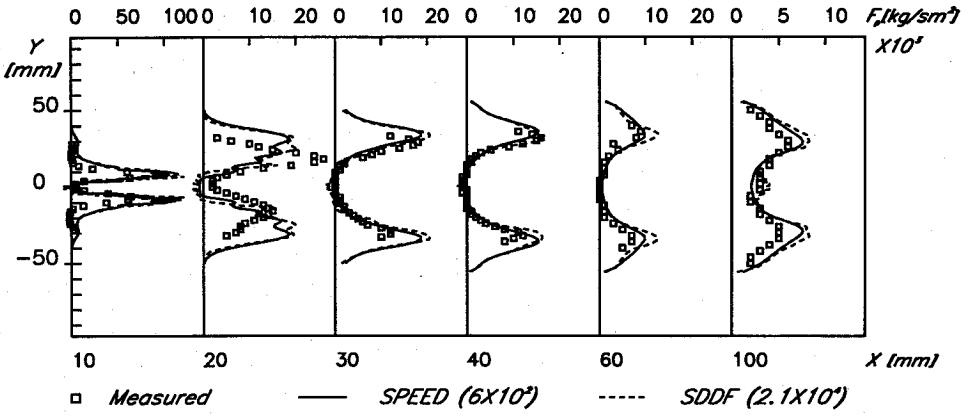

Fig. 13 Comparison of droplet mass flux.

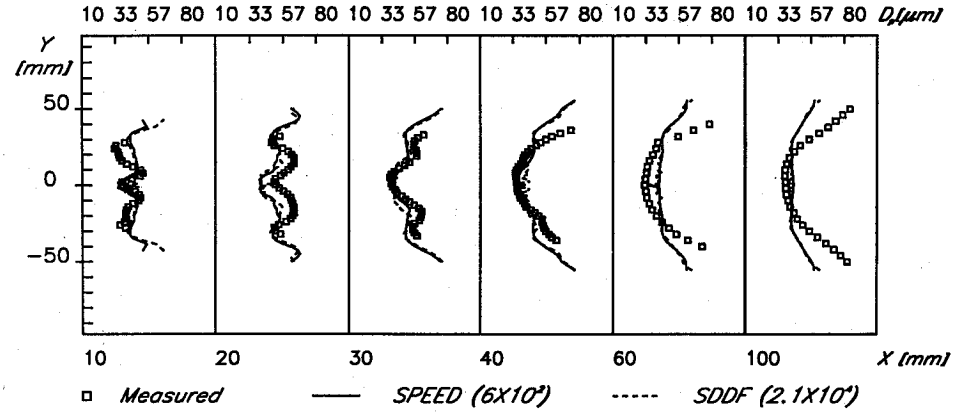

Fig. 14 Comparison of droplet mean diameter.

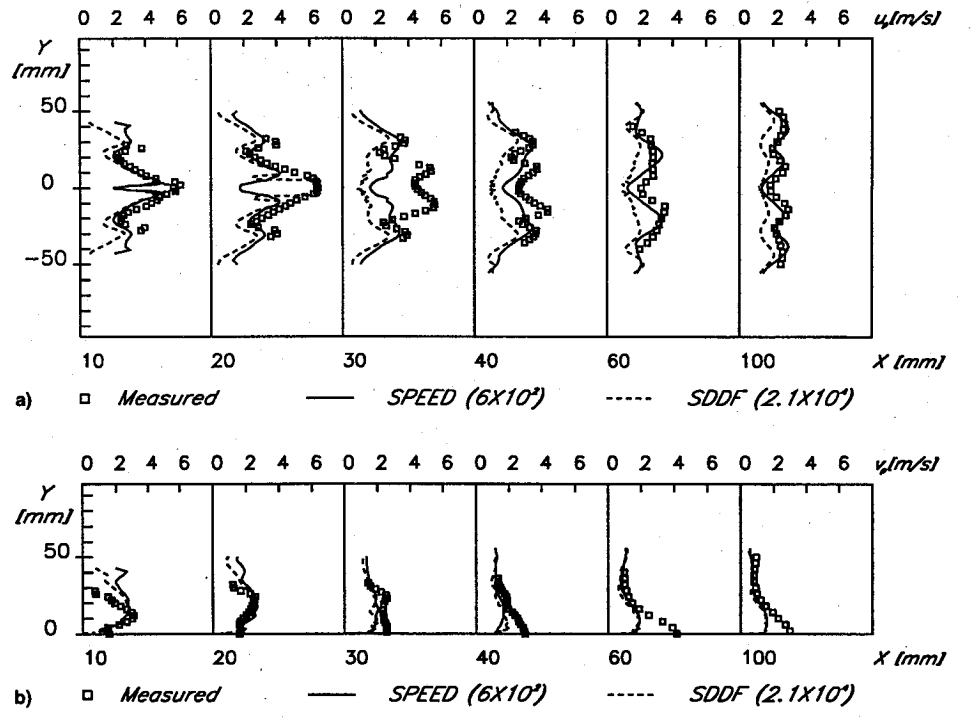

Fig. 15 Comparison of droplet fluctuating velocities: a) axial and b) radial rms.

should have minor effects on droplet properties in the region close to the inlet. Compared with the measurements, Fig. 11a is also indicative of the best predictions obtained with the SPEED model. A general underprediction of droplet mean diameters can be observed on the spray edge at $X = 100$ mm for all three models in Fig. 11b. However, numerical noise still persists in the predicted profiles of diameter with the SDWT and SDDF models. To have a clear idea of spray evolution, more profiles are presented as follows. For the sake of easier recognition, the SDWT model predictions are no longer shown. However, the detailed comparison of the SDWT and SDDF models can be found elsewhere.[23]

Shown in Figs. 12–14 are the profiles for the droplet axial mean velocity, number-mean diameter, and mass flux, respectively, at six stations. It can be seen that the SPEED model is generally superior to the SDDF model, even though 35 times as many of the droplet trajectories has been used in the SDDF model predictions. The satisfactory predictions with the SPEED model further enhances the belief that the dispersion width determined with Eq. (18) is appropriate for the SPEED model.

Finally, shown in Figs. 15a and 15b are the profiles of the predicted and measured droplet axial and radial fluctuating velocities, respectively. Even though slight discrepancies are present in the predictions of the radial fluctuating velocity, much better predictions of the droplet axial fluctuating velocity downstream have been achieved with the SPEED model (see Fig. 15a). The comparative study of Chen and Pereira[23] on the SDWT and SDDF predictions has shown that the predictions of the fluctuating velocities are very similar, both of which substantially underpredict the axial fluctuating velocity downstream of $X = 40$ mm. However, much improvement has been achieved with the present SPEED model, which clearly indicates the success of the present SPEED model. It should be stressed that the present SPEED model only considers the radial dispersion width along a droplet trajectory. It can be inferred that because of flow recirculations some further improvement could be achieved if the dispersion width in the streamwise direction has been accounted for.

Concluding Remarks

A SPEED model has been successfully developed for the prediction of turbulent two-phase flows. This model was first validated against a benchmark test, and was then applied to predict a polydispersed, turbulent, nonevaporating, hollow-cone spray in a strongly recirculating gas flow. In the present SPEED model, a memoryless Markovian-chain was used to determine the Lagrangian autocorrelation function, and a governing equation was derived to solve for the mean-squared dispersion-width. The developed SPEED model has ruled out the requirement of many repeated summing operations, unknown undersampling constant, and computer memory in the previous stochastic dispersion-width transport model. The present comparative study demonstrated that the SPEED model cannot only offer high computational efficiency, but also eliminate the numerical noise present in the conventional stochastic models when tracking a relatively few numbers of droplet trajectories. Moreover, the effects of the anisotropy of gas turbulence on droplet dispersion and the effects of droplet drift correction have also been accounted for in the SPEED model. Numerical results also demonstrated that, because of the unfavorable influence of strong flow recirculations, the conventional discrete delta-function model persistently produces some computational noise, even though thousands of droplet trajectories have been tracked. However, this does not affect the SPEED model predictions. The success with the SPEED model has made it possible that an accurate noise-free solution can be achieved by tracking only a very few number of droplet trajectories. Therefore, it can be concluded that the SPEED model should become a promising tool to efficiently predict turbulent two-phase flows of engineering significance. However, further improvement is still required to consider the dispersion effects in the streamwise direction.

Acknowledgment

The first author gratefully acknowledges the scholarship for postdoctoral research from the Portuguese Foundation JNICT under the Program PRAXIS XXI.

References

[1]Chigier, N. A., "The Atomization and Burning of Liquid Fuel Sprays," *Progress in Energy and Combustion Science*, Vol. 2, No. 2, 1976, pp. 97–114.

[2]Faeth, G. M., "Evaporation and Combustion of Sprays," *Progress in Energy and Combustion Science*, Vol. 9, Nos. 1–2, 1983, pp. 1–76.

[3]Crowe, C. T., "The State-of-the-Art in the Development of Numerical Models for Dispersed Phase Flows," *Proceedings of the International Conference on Multiphase Flows* (Tsukuba, Japan), 1991, pp. 49–59.

[4]Sirignano, W. A., "Fluid Dynamics of Sprays—1992: Freeman Scholar Lecture," *Journal of Fluids Engineering*, Vol. 115, Sept. 1993, pp. 345–378.

[5]Yuu, S., Yasukouchi, N., Hirosawa, Y., and Jotaki, T., "Particle Turbulent Diffusion in Dust Laden Round Jet," *AIChE Journal*, Vol. 24, No. 3, 1978, pp. 509–519.

[6]Gosman, A. D., and Ioannides, E., "Aspects of Computer Simulation of Liquid-Fuelled Combustors," AIAA Paper 81-0323, 1981.

[7]Sturgess, G. J., Syed, S. A., and McManus, K. R., "Calculation of a Hollow-Cone Liquid Spray in Uniform Airstream," *Journal of Propulsion and Power*, Vol. 1, No. 3, 1985, pp. 360–369.

[8]Shuen, J.-S., Solomon, A. S. P., Zhang, Q.-F., and Faeth, G. M., "Structure of Particle-Laden Jets: Measurements and Predictions," *AIAA Journal*, Vol. 23, No. 3, 1985, pp. 396–404.

[9]Chen, X.-Q., and Pereira, J. C. F., "Numerical Prediction of Evaporating and Nonevaporating Sprays Under Nonreactive Conditions," *Atomization and Sprays*, Vol. 2, No. 4, 1992, pp. 427–443.

[10]Yule, A. J., Seng, C. A., Felton, P. G., Ungut, A., and Chigier, N. A., "A Study of Vaporizing Fuel Sprays by Laser Techniques," *Combustion and Flame*, Vol. 44, No. 1, 1982, pp. 71–84.

[11]Chen, X.-Q., Freek, C., and Pereira, J. C. F., "Experimental and Numerical Study of a Water Spray in the Wake of an Axisymmetric Bluff Body," *Journal of Experimental Thermal and Fluid Sciences* (to be published).

[12]Mostafa, A. A., Mongia, H. C., McDonell, V. G., and Samuelsen, G. S., "Evolution of Particle-Laden Jet Flows: A Theoretical and Experimental Study," *AIAA Journal*, Vol. 27, No. 2, 1989, pp. 167–183.

[13]Adeniji-Fashola, A., and Chen, C. P., "Modeling of Confined Turbulent Fluid-Particle Flows Using Eulerian and Lagrangian Schemes," *International Journal of Heat and Mass Transfer*, Vol. 33, No. 4, 1990, pp. 691–701.

[14]Bulzan, D. L., Levy, Y., Aggarwal, S. K., and Chitre, S., "Measurements and Predictions of a Liquid Spray from an Air-Assist Nozzle," *Atomization and Sprays*, Vol. 2, No. 4, 1992, pp. 445–462.

[15]Chang, K.-C., Wang, M.-R., Wu, W.-J., and Hong, C.-H., "Experimental and Theoretical Study on Hollow-Cone Spray," *Journal of Propulsion and Power*, Vol. 9, No. 1, 1993, pp. 28–34.

[16]Chen, X.-Q., and Pereira, J. C. F., "Computation of Turbulent Evaporating Sprays with Well-Specified Measurements: A Sensitivity Study on Droplet Properties," *International Journal of Heat and Mass Transfer*, Vol. 39, No. 3, 1996, pp. 441–454.

[17]Litchford, R. J., and Jeng, S.-M., "Efficient Statistical Transport Model for Turbulent Particle Dispersion in Sprays," *AIAA Journal*, Vol. 29, No. 9, 1991, pp. 1443–1451.

[18]Chen, X.-Q., and Pereira, J. C. F., "Efficient Lagrangian Stochastic Transport Modeling of a Turbulent Evaporating Spray," 8th International Symposium on Transport Phenomenon in Combustion, San Francisco, CA, July 1995.

[19]Vames, J. S., and Hanratty, T. J., "Turbulent Dispersion of Droplets for Air Flow in a Pipe," *Experimental Fluids*, Vol. 6, No. 2, 1988, pp. 94–104.

[20]Chen, X.-Q., and Pereira, J. C. F., "Prediction of Evaporating Spray in Anisotropically Turbulent Gas Flow," *Numerical Heat Transfer*, Vol. 27, Pt. A, 1995, pp. 143–162.

[21]Berlemont, A., Desjonqueres, P., and Gouesbet, G., "Particle Lagrangian Simulation in Turbulent Flows," *International Journal of Multiphase Flow*, Vol. 16, No. 1, 1990, pp. 19–34.

[22]Litchford, R. J., and Jeng, S.-M., "Probability Density Function Shape Sensitivity in the Statistical Modeling of Turbulent Particle Dispersion," *AIAA Journal*, Vol. 30, No. 10, 1992, pp. 2546–2549.

[23]Chen, X.-Q., and Pereira, J. C. F., "Numerical Study of a Nonevaporating Polydispersed Turbulent Hollow-Cone Spray," 2nd International Symposium of Numerical Methods for Multiphase Flows, San Diego, CA, July 1996.

[24]Laufer, J., "The Structure of Turbulence in Fully-Developed Pipe Flow," NACA Rept. 1174, 1954.

[25]Bachalo, W. D., and Houser, M. J., "Evolutionary Behavior of Sprays Produced by Pressure Atomizer," AIAA Paper 86-0296, 1986.

[26]Rangel, R. H., and Sirignano, W. A., "An Evaluation of the Point-Source Approximation in Spray Calculations," *Numerical Heat Transfer*, Vol. 16, Pt. A, 1989, pp. 37–57.

[27]Durão, D. F. G., and Pereira, J. C. F., "Calculation of Isothermal Turbulent Three-Dimensional Free Multijet Flows," *Applied Mathematical Modeling*, Vol. 15, July 1991, pp. 338–350.